JOURNAL OF OPTOELECTRONICS AND ADVANCED MATERIALS Vol. 9, No. 6, June 2007, p. 1665 - 1670

Study of the structure of wear resistant thermal sprayed coatings on low alloy steels

V. KATENIDIS, D. CHALIAMPALIAS, N. PISTOFIDIS, G. VOURLIAS*, E. PAVLIDOU, A. STERGIOU, G. STERGIOUDIS
Department of Physics, Aristotle University of Thessaloniki, 54124 Thessaloniki, Greece

Low carbon steels, although they are characterized by high mechanical strength, good workability and low cost, they are prone to corrosion. Furthermore their surface is rather soft and as a result wear is often observed. For that purpose they are usually coated with other materials which do not affect their mechanical behavior but significantly improve their superficial properties. In the present work the structure of different coatings used for wear protection is examined with scanning electron microscopy, optical microscopy and X-ray diffraction. The deposition method was powder combustion thermal spray. The as received coatings are composed by several phases in the form of inclusions dispersed in a homogeneous matrix.

(Received November 14, 2006; accepted April 26, 2007)

Keywords: Thermal spray, Coatings, Wear, Metals and alloys, X-ray techniques, Electron microscopy

1. Introduction

Flame spraying is used for the application of a wide variety of feedstock materials including metal wires, ceramic rods, metallic and nonmetallic powders. In this technique the feedstock material is fed continuously to the tip of the spray gun where it melts in a fuel gas flame. As the materials are heated, they are changed to a plastic or molten state, accelerated by a compressed gas stream and propelled to the substrate. The particles strike the substrate, flatten and form thin platelets (splats) that conform and adhere to the irregularities of the substrate and to each other. As the sprayed particles impinge upon the surface, they cool down and build up, splat by splat, into a laminar structure forming this way the thermal spray coating [1-9].

The as-formed coating is not homogenous and it is typically characterized by a certain degree of porosity. Furthermore in the case of sprayed metals the coating contains oxides of the same material [1-9]. The bond between the substrate and the coating may be mechanical, chemical, or metallurgical or a combination of these, while the properties of the applied coating depend on the feedstock material, the thermal spray process, the application parameters (temperature etc) and post treatment of the applied coating [1-9]. All these parameters, along with the bond between the coating and the substrate, affect the microstructure of the coating which in turn determines its macroscopic properties.

The aim of this work was the study of the morphology and the microstructure of different flame sprayed coatings used for wear protection. Their examination was focused on the prediction of their mechanical properties and especially their hardness, since this is the main factor that affects wear resistance. This information could be of great significance for the determination of the limits of these coatings and for the improvement of their properties through rational choices.

2. Experimental procedure

Commercial, hot-rolled low carbon steel sheets SAE 1010 were sized (50×70×4 mm^3) and used as substrates. The specimens were cleaned with sandblasting prior to the coating process, which took place with a 5P-II Sulzer-Metco combustion powder spray gun. A schematic drawing of the layout of the deposition equipment is presented in Fig. 1. The feedstock of the spray gun was Metco powders as listed in Table 1. The spray parameters which were used are summarized in Table 2.

For the examination of the surface morphology of the coatings the samples were photographed with a Zeiss M8 stereoscope at low magnification. Afterwards, for the examination of the microstructure and the thickness measurements, cross sections from each specimen have been cut and polished up to 5 μm alumina emulsion. Initial observations of the polished samples have been made using a 20 kVolt JEOL 840A scanning electron microscope (SEM). The chemical composition of the observed surface was determined with an OXFORD ISIS 300 Energy Dispersive X-Ray Spectroscopy (EDS) analyser associated with the SEM and the related software in order to perform point microanalysis, linear microanalysis or chemical mapping of the surface under examination. The nature of the phases has been determined with X-ray diffraction (XRD) using a 2-cycles SEIFERT 3003 TT diffractometer (CuK_α radiation).

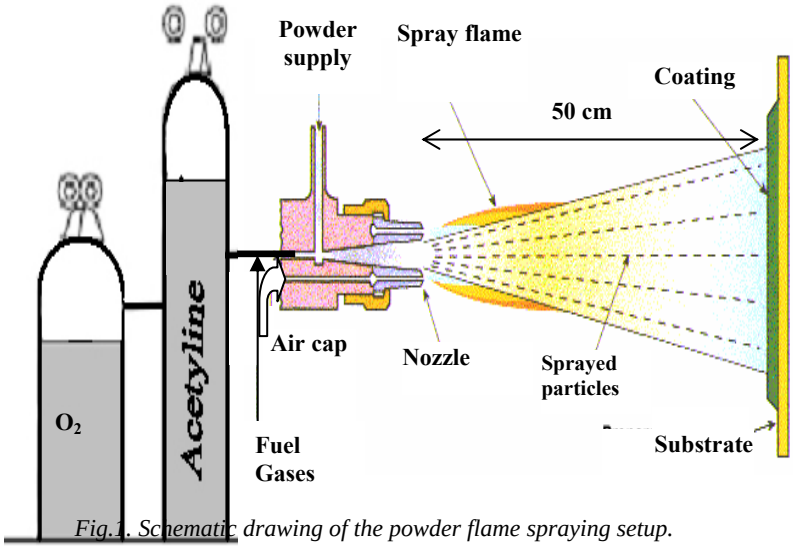

Fig.1. Schematic drawing of the powder flame spraying setup.

Table 1. Size and chemical composition of feedstock powders.

Metco powder	Composition	Particle size
15E	$Ni_{17}Cr_4Fe_4Si_{3.5}BC$	-106 +45 μm (-140 +325 mesh)
101NS	$Al_2O_3{\cdot}3TiO_2$	-45 +11 μm (-325 mesh +11 μm)
447NS	$Ni_5Mo_{5.5}Al$	-90 +45 μm (-170 +325 mesh)
12C	$Ni_{10}Cr_{2.5}B_{2.5}Fe_{2.5}Si_{0.15}C$	-125 +45 μm (-120 +325 mesh)

Table 2. Thermal spray conditions.

Parameter	Unit	Range
Spray distance	cm	50
Oxygen flow rate	l/min	43
Acetylene flow rate	l/min	19
Air flow rate	l/min	775

3. Results and discussion

As it was mentioned before, feedstock powders used for wear resistant coatings are 15E, 101NS and 12C. The morphology and the structure of each coating formed with these powders are expected to be different. In order to acquire a preliminary macroscopic estimation of the as received coatings the samples were photographed using stereoscope. Fig. 2 presents representative plain view photos of the surface of the flame sprayed samples. It is easily distinguished that all three samples are characterized by extremely rough surface. Due to the low magnification of the instrument, no further conclusions could be drawn from this examination.

In order to have a better aspect of the surface morphology and the coating thickness, plain view and cross section SEM micrographs were taken from the specimens. In every case the superficial roughness is obvious (Fig. 3). This surface morphology is common for thermal sprayed coatings. It is a result of the solidification of the metal droplets during their flight from the gun nozzle to the substrate. As a result solid spheres are stacked on the substrate surface. It usually depends on the powder particle size and the momentum of the particles when they hit the substrate. Finally the substrate morphology plays a crucial role on the coating morphology as solidified particles tend to follow its roughness [10].

From the cross section micrographs (Fig. 3b, 3d, 3f) the coating thickness was measured in every case from 250 to 300μm. From the same micrographs the boundaries of the lamellae formed from the sprayed droplets can be easily distinguished. The main characteristic of the examined coatings is the large porous areas which are located through the whole surface and whole mass of the coating. The formation of these pores is an inherent feature of the flame sprayed coatings as it is a result of the deposition mechanism. The droplets arrive on the substrate in a semi-molten state and consequently they collide in form of stacking spheres forming several voids among them which consist the porous areas of the coating [11, 12]. These porous areas can be restricted by altering some of the spraying parameters such as the gun-substrate distance or reheating the sprayed surface at the flame temperature, which could change the coating morphology.

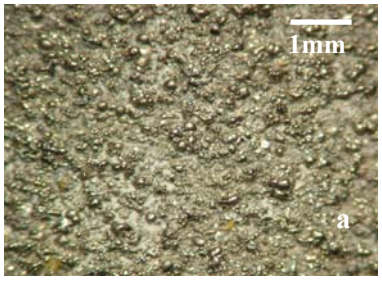

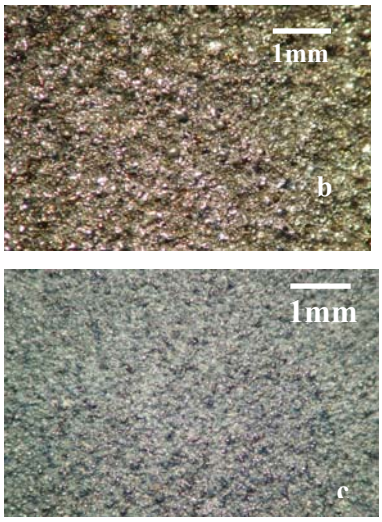

Fig. 2. Stereoscopic photographs of the surface of the coatings formed with powders 15E(a), 12C(b), 101NS(c).

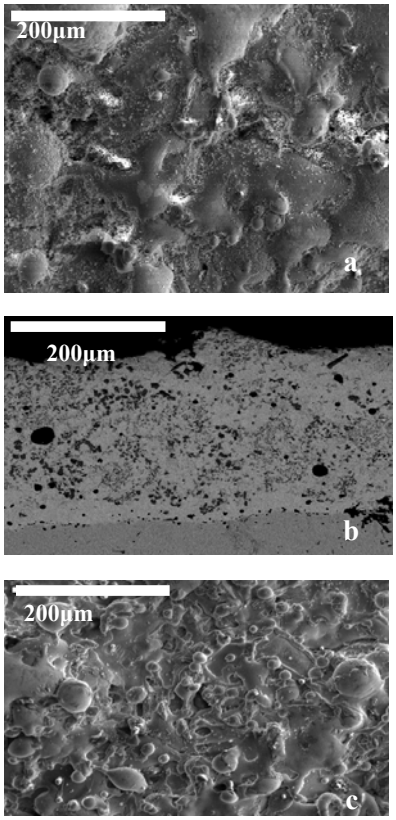

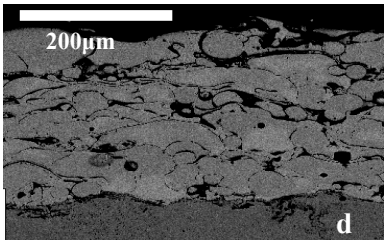

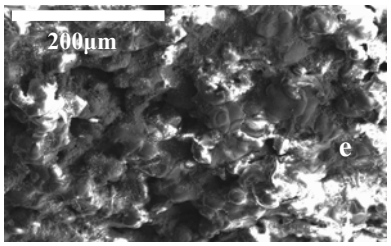

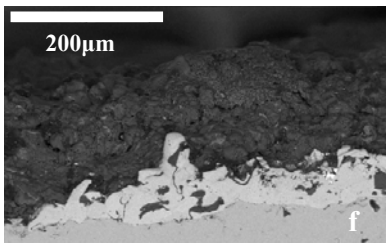

Fig. 3. SEM plain view (upper row) and cross section (lower row) micrographs of the coatings formed with powders 15E(a, b), 12C(c, d), 101NS(e, f).

EDS analysis of the 15E coatings revealed the existence of Si, Cr and Ni in the compositional profile taken by the total width of the cross-sectional sample (Fig. 4). Silicon is dispersed all along the coating in small amounts. Also there are localized areas that contain big amounts of nickel and no chrome. On the other hand there are also localized areas that contain only chrome and not at all nickel. Chrome areas can be distinguished as black spots in the SEM micrograph of Fig. 3b. Apart from the presence of the previously mentioned elements in the sprayed coating, oxygen amounts were recorded, due to the presence of several oxides trapped in the mass of the coating. Chemical mapping coming of this sample show clearly the Ni, Cr and Si distribution in the mass of the coating (Fig. 5). Also there is not any diffusion of the sprayed elements in the substrate. Hence only a mechanical bond is established between the substrate and the coating.

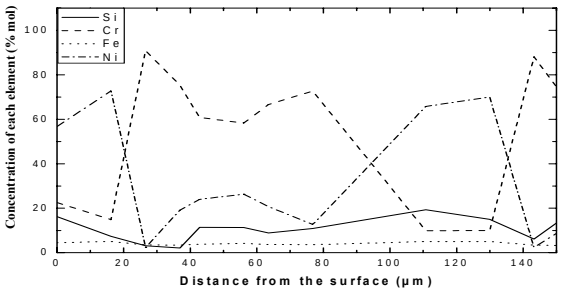

Fig. 4. Compositional profile along the cross section of 15E coatings.

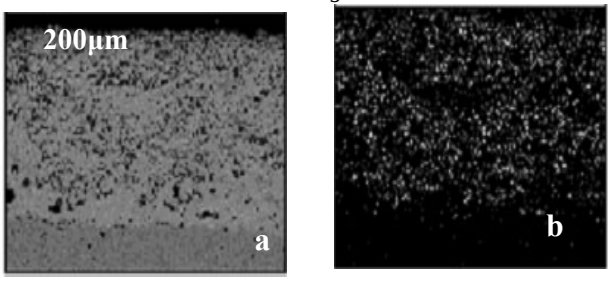

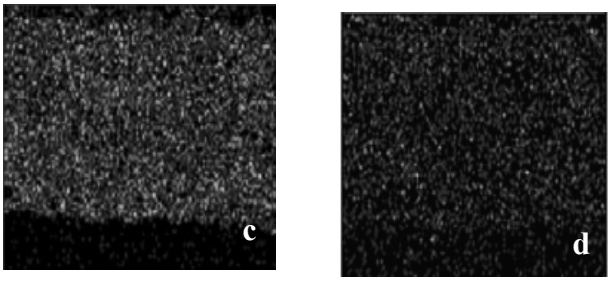

Fig. 5. Chemical mapping photos of 15E coatings (a) for Cr (b), Ni (c) and Si (d) elements.

XRD patterns taken from the same coatings (Fig. 6) revealed the existence of nickel (PDF#65-0380) and several Ni base phases as nickel is the matrix element of the coating. With the aid of PDF files it was found that picks correspond to Cr_3Ni_2 (PDF#26-0380), Fe Ni_3 (PDF#38-0419), Ni-Cr-Fe (PDF#33-0945) and Ni-Cr-Si (PDF#31-0405) phases [13]. The presence of these phases, particularly Fe Ni_3, make the coating wear resistent, because of their high hardness.

EDS analysis of the 12C coatings revealed the existence of Cr, Fe and Ni in the compositional profile taken from the cross-section of the sample. It was found that nickel is the main element of the coating. Cr is dispersed in the coating at small amounts in localized areas. In these areas the amount of nickel is significantly low which is obvious from chemical mapping of the coating (Fig. 7) and the EDS line scanning (Fig. 8). Also in this case a mechanical bond exists between the sprayed powder elements and the substrate as there is any diffusion been observed in the ferrous substrate.

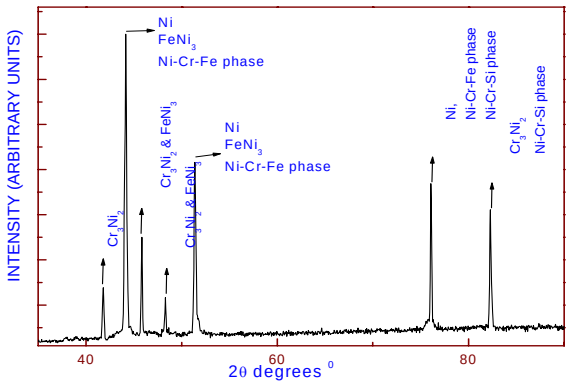

Fig. 6. XRD pattern of 15E coatings.

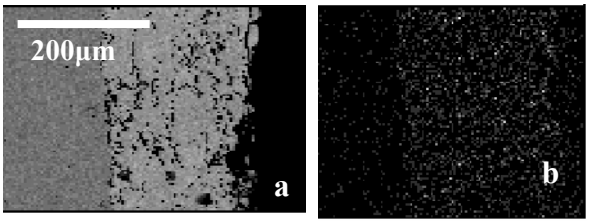

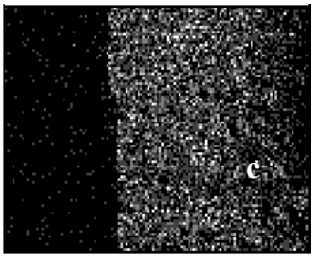

Fig. 7. Chemical mapping of 12C coating (a) for Cr(b), Fe(c) and Ni(d).

XRD patterns taken from the same coatings (Fig. 9) revealed the existence of several B-Cr phases (PDF#65-1357)[13] and the $Ni_{2.9}Cr_{0.7}Fe_{0.36}$ phase (PDF#33-0945) [13]. With the aid of PDF files these phases are denoted in the xrd diagram of Fig. 9. The reason why the presence of oxides was not distinguished with XRD analysis is because of their low concetration and also because reflections coming from the previous refered phases have very strong intensity not letting peacks of lower intesity to be visible.

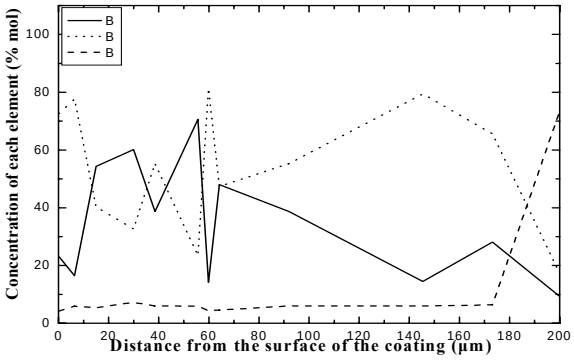

Fig. 8. EDS analysis of the compositional profile taken from the cross section 12C coatings.

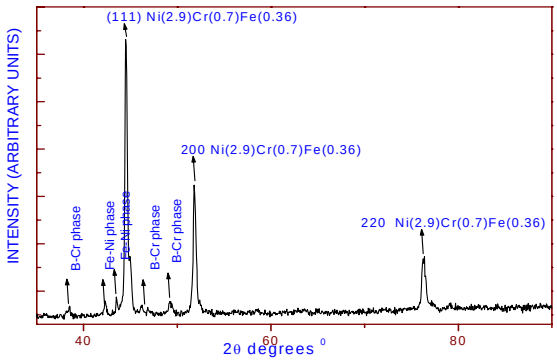

Fig. 9. XRD pattern of 12C coatings.

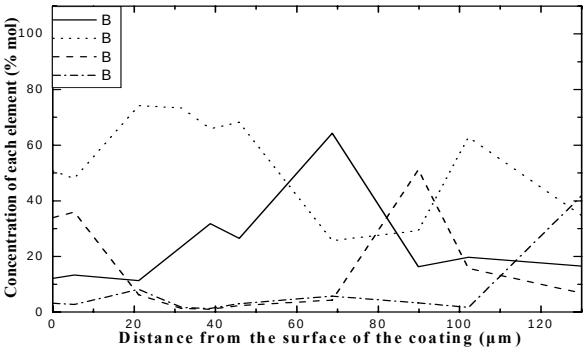

Fig. 10. EDS analysis of the compositional profile taken from the cross section 101NS coatings.

In order to ensure good adhesion of sprayed 101NS powder on the ferrous substrate there was 447NS powder sprayed before the main thermal spray procedure. So EDS analysis of the 101NS coatings revealed the existence of Al, Ni, Ti and O compounds in the compo-sitional profile taken by the total width of the cross-sectional sample (Fig. 10). As it was expected a two layered coating was formed. The first one, in contact with the substrate contains only nickel coming from 447NS powder which was primarily sprayed, and the second layer (outer layer) contains amounts of Al, Ti and oxygen coming from 101NS powder which was sprayed afterwards. These layers are easily distinguished in Fig. 3f as the bright area is the coating formed from 447NS powder and the dark layer is formed from the 101NS powder. We can safely claim that areas containing big amounts of Ti have low Al concentration and reversely. Finally there is no diffusion of the two layers as nickel is not traced o the upper parts of the whole coating. This is also obvious in the chemical mapping photos coming from this sample where the distribution of Ni, Al, Ti and O is reflected (Fig. 11). XRD patterns taken from the same coatings (Fig. 12) revealed the existence of Al_2O_3(PDF#75-1863) and Ti_3O_5 (PDF#09-0309) [13]. These phases are clearly denoted in the xrs pattern of Fig. 12.

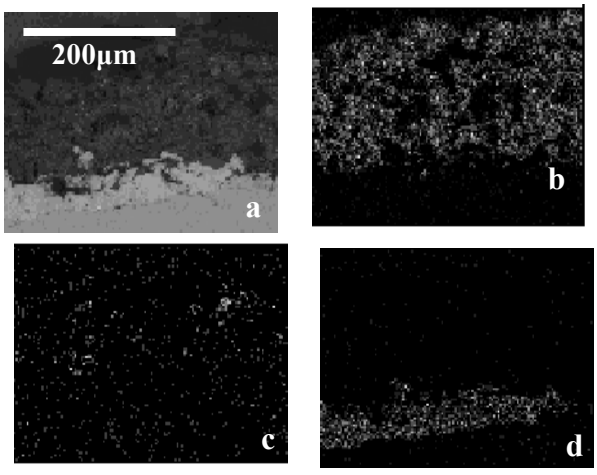

Fig. 11. Chemical mapping photos of 101NS coatings (a) for Al (b), Ti (c), O (d) and Ni (d) elements.

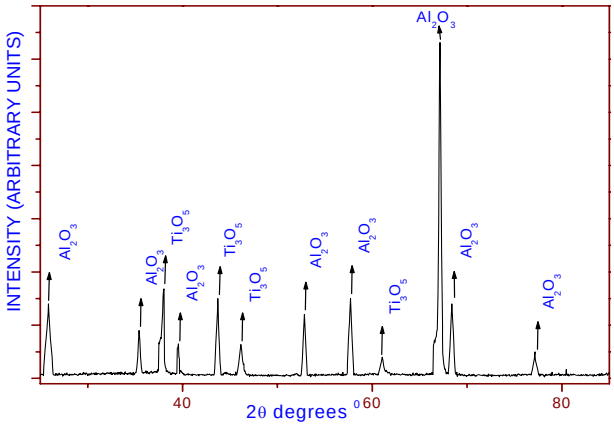

Fig. 12. XRD pattern of 101NS coatings.

4. Conclusions

In the present work thermal sprayed wear resistant coatings were studied. From this investigation it was concluded that:

- Every coating is covered by a very rough surface. Its cross-section is characterized by a large pore density as a result of the coating mechanism and the rapid cooling of the sprayed material.

- In every case there is a mechanical bond between the coating and the substrate as there is no diffusion of the substrate elements in the coating and no diffusion of the coating elements in the substrate.

- Coatings coming from 15E powder consists of Ni, Cr_3Ni_2, Fe Ni_3, Ni-Cr-Fe and Ni-Cr-Si phases. The existence of the phase's elements was also verified from EDS analysis.

- Coatings coming from 12C powder consists several B-Cr phases and the Ni(2.9)Cr(0.7)Fe(0.36) phase. EDS verified also the presence of oxygen in the coating mass and consequently the presence of oxides. However these oxides were not recorded with XRD because of their low concetration.

- Coatings coming from 101NS powder consist of of Al_2O_3 and Ti_3O_5 as it was revealed with XRD.

References

[1] P. Maass, P. Peissker, Handbuch Feuerverzinken, Wiley-VCH (1993).
[2] ASM Handbook, Vol. 6-Surface Treatments, ASM, New York (1999).
[3] ASM Handbook, Vol. 5-Surface Engineering, ASM, New York (2000).
[4] Engineer Manual 1110-2-3401, Thermal spraying: new construction and maintenance, USACE, 1999.
[5] ASM Handbook, Vol. 7-Thermal Processes, ASM, New York (1998).
[6] ASM Handbook, Vol. 5-Surface Engineering, ASM, New York (2000).
[7] M. L. Thorpe, Adv. Mater. Process. **143**, 50(1993).
[8] B. Walser, SPRAYTIME **10**, 1(2004).

[9] J. Read, International Thermal Spray Association, Keynote address, China International Thermal Spray Conference and the 16th National Thermal Spraying Seminar, Dalian, China, 22–25 Sept 2003
[10] Y. Chen, G. Wang, H. Zhang, Thin Solid Films **13,** 390 (2001).
[11] ASM Handbook, Vol. 13-Surface Treatments, ASM, New York (1996).
[12] H. Herman, S. Sampath, R. McCune, Mat. Bull. **5**, 17(2000).
[13] PC Powder Diffraction Files, Version 2.02, JCPDS-ICDD, 1999.

*Corresponding author: gvourlia@auth.gr